



OPEN Fire effects on phytolith carbon sequestration

Rencheng Li^{1,2}✉, Zhitao Gu¹, Richard S. Vachula³, Haiyan Dong¹✉, Mengtong Xu¹, Xiaofang Chen¹, Bin Xu¹ & Yunwu Sun¹

Phytolith have been recognized as an important soil bioavailable Si source for plants, as well as a sink of C and heavy metals in soils. Though the impacts of fire and heat on phytolith sequestration of some nutrients (phosphorus, potassium) and heavy metals have been addressed, little attention has been paid to fire's effects on phytolith carbon sequestration. In this study, the carbon and dissolved Si content of phytoliths extracted from 6 common grass species and their burned ashes, as well as phytoliths collected from different areas (burned, transitional, and unburned) of a pine forest, were compared to characterize the effects of open fire on phytolith carbon content, solubility, and carbon sequestration. The carbon content and Si dissolution of ashed phytoliths varied between plant species, and differed with phytoliths from modern plants. The topsoil phytoliths had increased carbon content, and generally decreased solubility across the gradient of unburned, transitional, and burned pine forest. We therefore conclude that open fire can cause changes in phytolith related carbon content and solubility, as well as its preservation in soils. This study provides new perspective on the effects of open fire on phytolith carbon sequestration and its estimation.

Keywords Phytolith, Dissolved silicon, Carbon sequestration, Fire

Natural fires can have severe impacts on ecosystems, including the alteration of ecosystem productivity, biodiversity, and functioning, which often impact soil biogeochemistry, plant communities, human health, and animal populations^{1,2}. Investigation and monitoring of fire effects on ecosystem elements like biodiversity, runoff, water quality and water supply^{3,4}, as well as soil composition and nutrition^{5,6}, can provide the basis for ecosystem restoration and management decisions. Soil composition and nutrition changes due to fire are often attributed to the input of fire-derived ashes composed of charcoal, phytolith, and mineral elements. The biogeochemical effects of fire ash on major elements such as C, N and P have been broadly studied across various climate regions⁷. Black carbon has a longer residence time in soil than non-burned C is thus considered to act as a long-term C sink⁷. SiO₂ is an important component of ash, accounting for example for approximately 56.2% of rice straw ash by weight⁸. Phytolith is primarily composed of SiO₂ and H₂O, but also contains smaller organic components and various inorganic mineral elements^{9,10}.

In recent research, phytolith has been recognized as an important bioavailable Si source of soil, as well as an overlooked mechanism of C and heavy metal sequestration in soils^{11–16}. Heat has an important influence on the dissolution properties of phytolith by affecting organic removal and surface modification, which alters elemental cycling in phytolith^{12,17}. Therefore, an increasing number of studies have focused on the effects of fire and heat on the chemical composition and dissolution properties of phytolith.

The physical and chemical properties of phytoliths might be altered by fire and heat. The physical features of phytolith (e.g. morphology, colour and opacity, refractive index, auto-fluorescence and molecular surface properties detectable by Raman spectroscopy and auto-fluorescence) are shown to change when subjected to high temperatures^{18–22}. Burning of plant tissue activates simultaneous and successive processes, e.g., dehydration, decomposition, carbonization, volatilization and crystallization, which target organic matter, silica, or their associated substances. These processes could cause some heavy metal elements (As, Pb, Zn) to become encapsulated and/or absorbed with silica phases^{14,17,23}. Upon heating to temperatures above 200°C water molecules start to form from the surface hydroxyl groups of phytolith. The hydroxyl groups are completely stripped off at 600°C²⁴. Phytoliths contain small amounts of organic components termed phytOC (phytolith occluded carbon) which ranges from 0.1 to 5.8%^{16,25–29}. Phytoliths that have been exposed to fire often become darkened in color as compared to clear, unburned phytoliths^{18,19,28,30}. The darkened color of burned phytoliths is probably derived from the oxidation of phytolith-occluded carbon (PhytOC)¹⁸. However, some authors have

¹College of Earth Science, Guilin University of Technology, Guilin 541004, China. ²Guangxi Key Laboratory of Hidden Metallic Ore Deposits Exploration, Guilin 541004, China. ³Department of Geosciences, Auburn University, Auburn, AL 3684923187, USA. ✉email: lirencheng_xie@163.com; 1875864792@qq.com

proposed that the darkened color is not generated from the occluded carbon in phytoliths but rather that black carbon is adsorbed by phytoliths exposed to open flames^{21,28}.

As phytoliths are important sources/carriers of nutrients (e.g., K and P)^{12,31}, a fast-reacting Si source for soils and crops^{32,33}, a notable tool of archaeobotany and paleoenvironmental reconstruction^{9,34,35}, and important agents for the sequestration of organic matter and CO₂^{13,36–38}, it is worthwhile to know how fire affects the dissolution of phytoliths. Phytolith solubility links to phytolith preservation in soils and sediments, as well as the cycling of elements in phytolith^{39–41}. Fire/heat can change their solubility^{12,17,39}. The effect of fire on phytolith solubility is related to temperature, phytolith elemental compositions, morphotypes and the plant species from which the phytolith are produced. When temperature increases, crystallization of silanol groups will form siloxane bonds, making the surface hydrophobic. This reaction reduces adsorption of water molecules on the surface and prevents the breakage of the surface siloxane bonds^{12,42}. High treatment temperature can result in a re-arrangement and crystallization of silica in phytolith, decreasing its solubility. The release of Si and other elements (such as Si, K, P, Pb, As) in rice straw ash (treated in a muffle furnace) and biochar from pyrolysis increases with increasing treatment temperature. This is likely because the decomposition of organic matter increases the surface exposure of phytolith silica and thereby decreases its protective role (surface coverage, hydrophobicity). But, it is also likely a tradeoff beyond a certain temperature because of the increased crystallization of phytolith. Phytolith affected by fire and heat have different dissolution properties as a result of their variable chemical and physical forms^{11,12,17,31,38}. The phytoliths of wheat extracted by dry ashing in a muffle furnace at 500 °C were less stable than unburnt phytoliths, and different morphotypes dissolved rather un-uniformly³⁹. Soil organic matter collected from spruce, beech forest and peat were treated in a furnace at 350 °C and 500 °C to obtain black carbon and white ash, respectively, and their Si releases were compared. The Si release data showed fire can enhance solubility of biogenic silica⁴³.

Together, these observations led to the hypothesis that fire could have effect on phytolith carbon sequestration by changing its solubility and carbon content. To date, the transformation, morphology, and dissolution of phytolith affected by fire and heat have not been comprehensively addressed. Biochar, which is mainly comprised of phytolith, is a major component of the geological Si–C cycle⁴⁴. Phytolith occluded carbon (PhytOC) is considered as a form of long-term carbon sequestration in soils²⁵. Previous dissolution experiments showed that phytolith mixed with ash (produced from organic matter ashed in a furnace), black carbon, and/or soil brought exogenous and secondary silicon to be involved in the dissolution process^{12,17,39,43}. Little is known about the effect of open fire on the carbon content and solubility of pure phytolith^{28,39}, or what happens to this occluded carbon during vegetation fires⁴⁵. Although the darken color of burned phytolith is probably resulted from adsorption of black carbon²⁸, it is unclear how the adsorption of carbon influences the phytolith carbon sequestration.

To unequivocally discern that fire effect on phytolith carbon sequestration, the carbon content and solubility of phytoliths extracted from 6 common grass species and their burned ashes are analyzed and compared to phytoliths collected from topsoils in a pine forest site burned by a forest fire, as well as transitional and unburned areas, to study the effect of open fire on phytolith carbon content, solubility, and carbon sequestration.

Materials and methods

Regional setting

Grass and topsoil samples were collected from the Guilin Institute of Agricultural Sciences, the Guangxi Institute of Botany (Chinese Academy of Sciences), and a burned area of pine forest in Huangshankou Village in the Lingui District of Guilin City (110°7'20"E, 25°14'56"N), respectively. Guilin City is located in southwest China (Fig. 1). It is in the subtropical monsoon climate region, and is affected by both the SW maritime monsoon from the Indian Ocean and the SE maritime monsoon from the western Pacific Ocean. It has an annual mean temperature of 18.8 °C and total annual precipitation of 1874 mm. The long-term lowest and highest monthly mean temperatures are 15.6 °C for winter and 23.0 °C for summer⁴⁶. Vegetation in the region is characterized by subtropical evergreen broad-leaved forest. The burned area sampled was on a mountain with an altitude less than 300 m. It has sandstone soil, and hosts a secondary coniferous forest composed of *Pinus massoniana* Lamb, *Quercus L. Cunninghamia lanceolata* (Lamb.) Hook (*Chinese fir*) and fern species. *Pinus massoniana* Lamb is the dominant plant species. Meanwhile, grass Panicoideae species, such *Imperata cylindrica* (L.) Beauv., *Miscanthus floridulus* (Lab.) Warb. ex Schum et Laut., and *Setaria palmifolia* (J.Koenig) Stapf. are widely distributed outside of forest stands. After the wildfire event occurred in 2021, the burned area's vegetation was dominated by ferns, as well as a few shrub and Panicoideae species.

Sampling and analysis

Sample preparation

About 500 g of mature leaves of 3 crops (rice, maize and sugarcane) and 3 common grasses were collected in December, 2020 (grass species are listed in Table 1). These six grasses are all common subtropical plant species. These 3 crops were experimental plants, and provided (identified by agro-technician Zhisi Shi) from Guilin Institute of Agricultural Sciences, and. Three wild grasses were collected in roadside in *Guangxi Institute of Botany, Chinese Academy of Sciences*. These three sampled grasses were transferred to the laboratory and submitted for identification by Professor Guangzhao Li (*Guangxi Institute of Botany, Chinese Academy of Sciences*). To maintain the representativeness of sampled leaves, they were obtained from more than 10 individual plants grown within a 10 m² area²⁸.

The sampling scheme of soil and sediment in the forest fire site is detailed by Wen et al.⁴⁷. Samples of soils and gully sediments were taken from different slope positions of the mountain on which pine forest was burned in Huangshankou Village. A sample was also taken from an unburned forest 1–2 km away from the fire perimeter as a control. The sample from the unburned area is not located downwind of where the fire occurred based

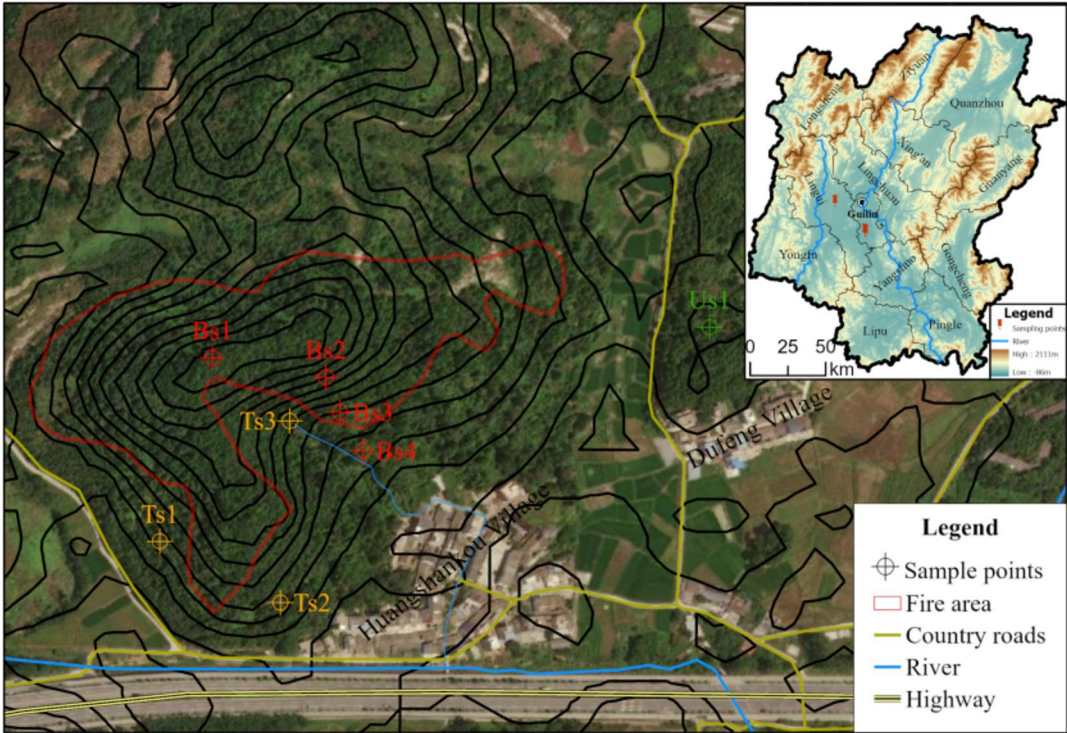


Fig. 1. Map of sampling locations(Satellite imagery comes from Esri, © OpenStreetMap contributors, TomTom, Garmin, Foursquare, METI/NASA, USGS).

Grass species	Subfamily	Genus	Sampling location
<i>Oryza latifolia</i> Desv.	Oryzoideae	<i>Oryza</i>	Guilin Institute of Agricultural Sciences (110°18'59"E, 25°4'19"N)
<i>Zeamays</i> L.	Panicoidae	<i>Zea</i>	
<i>Saccharum officinarum</i> Linn.	Panicoidae	<i>Saccharum</i>	
<i>Miscanthus floridulus</i> (Lab.) Warb. ex Schum et Laut.	Panicoidae	<i>Miscanthus</i>	Guangxi Institute of Botany, Chinese Academy of Sciences (110°18'35"E, 25°4'57"N)
<i>Setaria palmifolia</i> (Koen.) Stapf.	Panicoidae	<i>Setaria</i>	
<i>Imperata cylindrica</i> (L.) Beauv.	Panicoidae	<i>Imperata</i>	

Table 1. Descriptions of sampling grass species.

on the northeasterly prevailing wind direction. Samples were also taken from the transition area (Fig. 1), or the burned-unburned forest boundary, which spanned 200 m in this study⁴⁸. The sampled forest stands in the burned-unburned transition area have a similar vegetation type as the burnt forest stands that were sampled. The transitional samples were only collected in the southern direction because the burned mountain is surrounded by the village, and the other direction burned completely. All samples were taken using a 5-point sampling method (five points from four vertices and the diagonal intersection of a quadrilateral), and 1–2 cm thick topsoil subsamples of the five points were mixed to form one sample, so as to maintain sampling representativeness. The plant litters were removed from the topsoils before sampling from the transitional area and unburned area. A total of 8 samples were obtained from the burned, unburned, and transitional areas in 2021 (detailed information is provided in Table 2).

Phytolith extraction and classification

All collected plant leaves were cleaned, dried, and cut into less than 5 mm pieces before phytolith extraction. The leaves were divided into two parts, with one part being used to extract phytoliths (as unburned phytolith). The second part of the leaves were used for open burning to obtain ashed phytolith. All grass leaves were burned on tinfoil under open air conditions to generate ashes (at approximately 420 °C³⁸), the ashes were collected to extract ashed phytolith²⁸. The soil and sediment samples were dried in an oven (70 °C), then the roots were picked out prior to grinding samples. The dried and ground samples were passed through a 60-mesh screen (250 μm).

Phytoliths for carbon content and dissolution analyses were extracted using a microwave digestion method modified from Parr¹⁸ and Parr et al.²⁶. A relatively high temperature (200 °C) for the microwave digestion was chosen, and a two-step oxidation of phytolith with H₂SO₄ and K₂Cr₂O₇ was used²⁸. The specific steps of sample

Sample number	Sampling type	Topography	Vegetation
Bs1	Soil from burned area	On top of the hill	Pine, grass
Bs2	Soil from burned area	Slope	Pine, fern
Bs3	Soil from burned area	Valley	Pine, fern
Bs4	gully sediment from burned area	Valley, south of the burned area	
Ts1	Soil from transitional area	Slope, southwest of the burned area	Pine, fern
Ts2	Soil from transitional area	Slope, south of the burned	Pine, Quercus L.
Ts3	Soil from transitional area	Valley area	Pine, Quercus L.
Us1	Soil from unburned area	Slope, northeast of the burned area	Pine, fern

Table 2. Descriptions of forest sampling sites.

preparation were as follows: (1) Weigh cut plant leaves (~ 1 g), ashes (~ 0.5 g), and soil (sediment) (~ 5 g), and load each sample into the digestion tubes; (2) Add 15 ml HNO_3 (superior grade) into the tubes to start the first microwave digestion, (3) Add 5 ml HNO_3 (excellent grade pure) and 10 ml 30% H_2O_2 for the second digestion step (for microwave digestion system conditions, refer to Dong et al.²⁸), then transfer samples to centrifuge tubes and wash them with distilled water (at least 3 times, 2500 rpm, 5 min); (4) Add 2.5 ml concentrated H_2SO_4 and 2.5 ml $\text{K}_2\text{Cr}_2\text{O}_7$ (0.8 mol/L), heat the digestion vessel in a hot water bath (90 °C for 90 min) to test whether the extraneous organic material was removed completely, then wash with distilled water until the solutions are pH neutral. This step was repeated two times. (5) The ashed phytolith samples were separated into two subsamples. One subsample was bleached using NaClO_3 to monitor its influence on the darkened color of burned phytolith. The bleached samples were shaken every 12 h, and let to stand for 48 h. After this process, the samples were washed until the solutions pH values were neutral. The phytoliths obtained were termed 'ashed phytolith with bleaching' samples.

The phytoliths for morphology and assemblage analysis were extracted from ashes and soils (sediments) by using the wet ash method⁴⁹. The extraction follows these steps: the removal of organic matter by H_2O_2 , carbonates by HCl, and clay by decantation. A heavy liquid floatation extraction technique was applied for the soil samples.

The extracted samples were identified under a Leica DM2500 biomicroscope at a magnification of ×400. Phytolith purity (no visible organic matter in the matrix) was noted for each sample.

Phytolith morphology classification was conducted following published references^{47,50,51}. All morphotypes were named according to the International Code for Phytolith Nomenclature 2.0⁵².

Determination of phytolith carbon content

Carbon content in the phytolith samples was determined by an alkali-capacity spectrophotometry method⁵³. For each extracted phytolith sample, 0.8 mol/l potassium dichromate was used to examine the extraneous organic materials outside of the phytolith cells, and to ensure complete removal of organic matter^{54,55}. The specific steps are described by Li et al.²⁹ and are as follows: The dried phytolith (0.01 g) was put in a 10 ml PTFE tube, 0.5 ml NaOH (10 mol L^{-1}) was added and left for 12 h. The samples were transferred to colourimetric tubes. $\text{C}_6\text{H}_{12}\text{O}_6$ was used to prepare an organic C standard solution (0.90,909 g L^{-1}), with 0, 0.5, 1.0, 1.5, and 2.0 ml of the standard placed in colourimetric tubes and the volumes brought up to 2.0 ml with ultrapure water. 1.0 ml $\text{K}_2\text{Cr}_2\text{O}_7$ (0.8000 mol L^{-1}) and 4.6 ml H_2SO_4 were added to each phytolith sample and standard solution aliquots, and they were heated at 98 °C for 1 h. After cooling, all the samples were volumed to 25 ml and centrifuged (2500 r/min, 10 min). The supernatant of each sample and standard solution was placed into a 1 cm optical path cuvette, and the absorbance was measured at 590 nm using a photometer. The standard solution absorbances were used to plot a calibration curve and establish the regression equation to calculate the organic carbon content of the phytolith samples.

Determination of dissolved Si

CaCl_2 -extractable Si content (CaCl_2 -Si) is used to assess the bioavailable Si pool in soils^{40,56}. We measured it through a kinetic extraction using a solid: liquid ratio of 0.03 g:50 mL (0.01 M CaCl_2). For each sample, 30 mg of extracted phytolith powder was placed into an 80 ml plastic centrifuge tube. The phytoliths in the tube were shaken in 50 ml of CaCl_2 solution at 20 °C for 1, 3, 5, 7 and 14 days. At the end of each extraction, the content of Si was determined using the molybdate blue method^{57,58}. A reagent-blank experiment was also performed according to the aforementioned procedure. All analytical measurements were conducted in triplicate. The absorbance of samples processed was measured at 700 nm using a photometer. The absorbance data of standard Si solution were used to plot a calibration standard curve and calculate the content of DSi in the samples. The detailed experimental process is explained by Wang et al.⁵⁸.

Determination of dissolved Si

An Independent Samples t-test (95% Confidence interval) and Paired-Sample t-test were performed to assess the statistical significance of the difference between the carbon content of ashed and unburned phytolith samples, and topsoil phytolith from different area of forest fire, respectively. Linear regression analyses were performed to reveal the relationship between the release rate and time of phytolith dissolution. Statistical analyses were performed using SPSS 19.0 software.

Results

Phytolith morphology and assemblage

The six grass species produced different phytolith morphotypes and assemblages (see Supplementary Fig.S1). The darkened burned phytolith varied with phytolith morphotype and the plant species burned. There were no visible plant tissues or microcharcoal particles in the phytolith slides after microwave digestion, suggesting that the elimination of non-related carbon was robust and complete²⁸. The darkened color of burned phytolith became weakened after the bleaching process (Fig. 2).

The phytoliths in the forest topsoil were dominated by BLOCKY IRREGULAR, TABULAR ELONGATE UNSCULPTED, TABULAR IRREGULAR, and TRIANGULAR PRISMATIC and had relatively low proportions of BULLIFORM FLABELLATE, BILOBATE, ACUTE BULBOUS. BILOBATE had high proportions of GSSCP (Grass silica short-cell phytoliths) present. Few SPHEROID PSILATE, BLOCKY RIDGED, BLOCKY SCROBICULATE phytoliths were identified. Sediment samples from the burned area had higher proportions of BULLIFORM FLABELLATE, SADDLE, and ELONGATE relative to the soil samples. The transitional and unburned areas had higher proportions of BILOBATE phytolith than were present in the burned area. There were more micro-charcoal particles in samples from the burned area than the transitional and unburned areas (Fig. 3, Supplementary Fig.S2).

Phytolith carbon content

The phytolith occluded carbon (PhytOC) of the six modern plants ranged from 0.2 to 1.3%. The ashed phytoliths that were unbleached and bleached had carbon content values that varied between 1.1 and 2.8%, and 0.4–2.1%, respectively. The average carbon content present difference ($p=0.00$, $n=14$, Paired Sample t-test) between unburned and ashed phytoliths from these plant species. The carbon content of each individual plant species showed an increase trend from unburned phytolith (from modern plant) to ashed phytolith with bleaching, to ashed phytolith (Fig. 4).



Fig. 2. Burned and unburned phytoliths from six grass leaves. A: Unburned phytolith; B: Ashed phytolith with bleaching; C: Ashed phytolith. a: BULLIFORM FLABELLATE; b: BILOBATE; c: HAIR; d: RONDEL; e: ACUTE BULBOSUS; f: ELONGATE ENTIRE; g: ELONGATE DENTATE; h: SPHEROID PSILATE; i: Scale of field of view = 50 μ m.

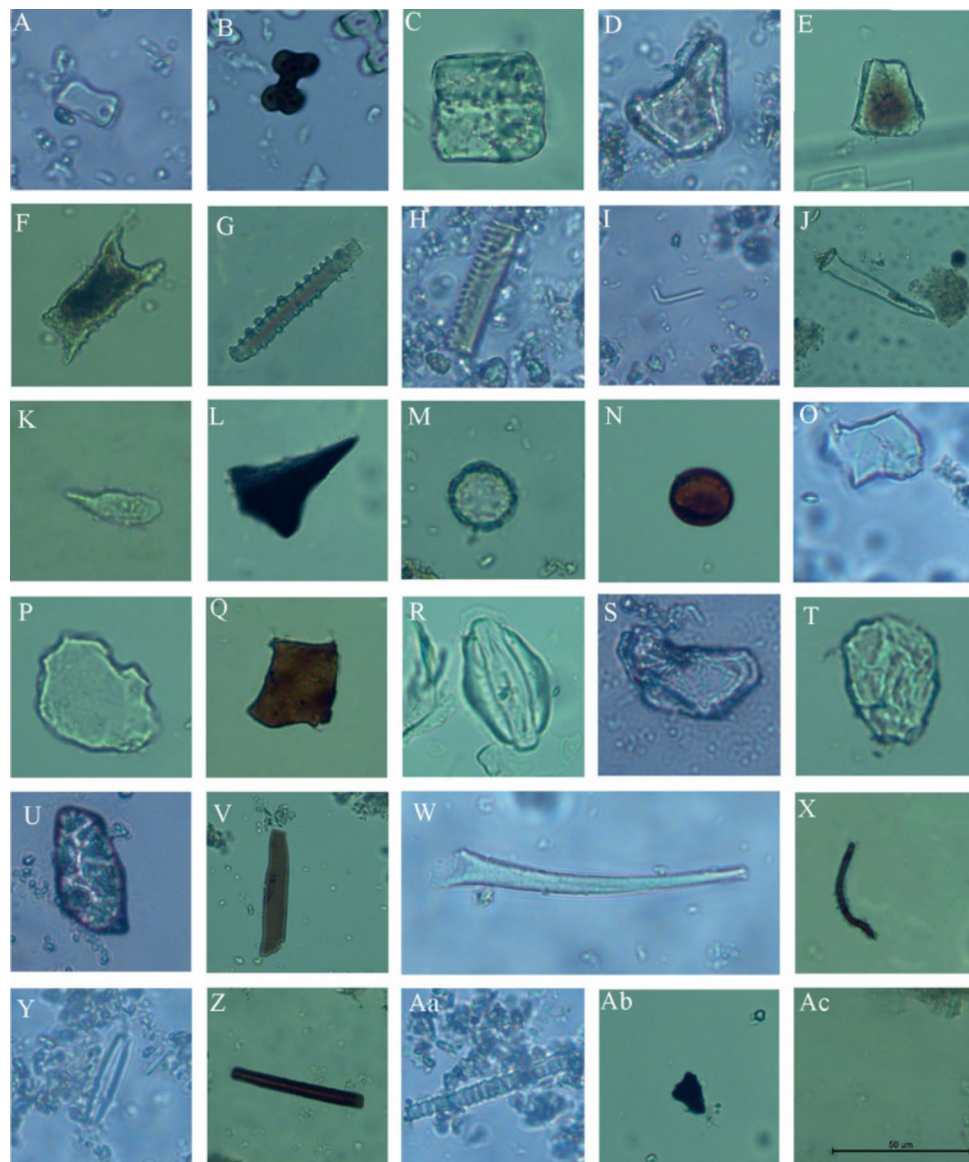


Fig. 3. A: phytolith morphotypes from forest topsoil samples. SADDLE; B: BILOBATE; C: CUBIC; D-E: BULLIFORM FLABELLATE; F: ELONGATE AMPLIATED ECHINATE; G: ELONGATE CAVATE TERMINAL; H: ELONGATE GRANULATE; I: HAIR; J: MACROHAIR; K-L: ACUTE BULBOSUS; M-N: SPHEROID PSILATE; O-Q: TABULAR IRREGULAR; R: STOMA; S: BLOCKY IRREGULAR; T: BLOCKY SCROBICULATE; U: BLOCKY RIDGED; V: TABULAR ELONGATE UNSCULPTED; W-X: SCLEREID; Y: TRIANGULAR PRISMATIC; Z: ELONGATE PSILATE; Aa: TRACHEARY ANNULATE; Ab: Charcoal; Ac: Scale of the field of view = 50 μ m.

The carbon contents of soil phytolith samples from the forest fire (burned) area ranged from 0.78 to 1.64%, and exhibited relatively higher values ($p=0.029$, $n=4$, An Independent Samples t-test) than those of samples from the transitional and unburned areas. The carbon content and microcharcoal concentrations were much higher in phytolith samples from burned areas than those from unburned and transitional areas (Fig. 5).

Dissolved silicon

The blank control sample showed very low DSi content across the time period of analysis, indicating that the samples were not contaminated during the experimental process. The dissolved Si concentrations increased with the progression of test days for all of phytolith samples. Across the dissolution period, the ashed phytoliths generally contained lower DSi contents relative to phytoliths from modern unburned plant leaves. As examples, the DSi content of ashed phytolith decreased from 49.85 to 17.39 mg/kg, and from 56.28 to 19.07 mg/kg, for *Oryza latifolia* Desv. and *Zea mays* L. on the 14th day, respectively. Nevertheless, phytoliths of *Saccharum officinarum* Linn. showed no apparent difference between ashed and unburned samples, and *Imperata cylindrica* (L.) Beauv. had increased DSi after the burned treatment as opposed to the same pattern produced by the

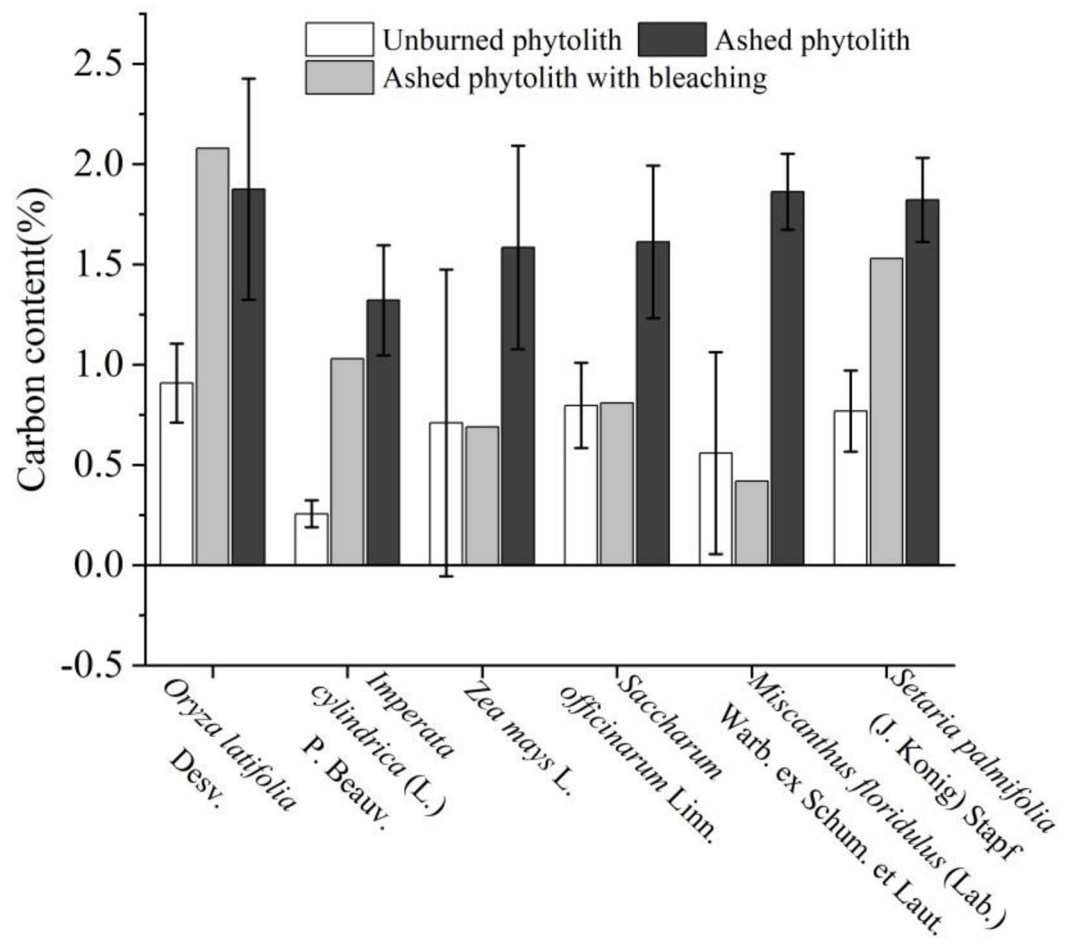


Fig. 4. Carbon content of phytoliths from 6 grass leaves varied with ashing (under open fire condition) and subsequent bleaching treatments.

unburned treatment for the other plants (Fig. 6, Supplementary Table S1). The slope coefficients of functions fitted to the relationships between DSi release of phytoliths from 6 grass leaves and CaCl_2 -extraction days ranged from 0.65 to 2.55. The range of these coefficients decreased from 0.27 to 1.03 with the implementation of the open combustion treatment (Fig. 6), showing the ashed phytolith procedure decreased the DSi release rate.

The phytoliths of topsoil samples from the burned area showed different release rates of Si. For example, sample Bs1 had the lowest release rate of Si content. The released silicon from forest fire (burned) and non-fire (transitional and unburned) areas increased as a function of the laboratory reaction time, though the unburned and transitional area phytoliths exhibited greater rates of silicon dissolution in the first five days (Fig. 7a, Supplementary Table S2). The slope coefficients of functions fit to the relationships between DSi release of soil phytolith and extraction days ranged from 1.50 to 1.63 for burned area samples, and from 2.22 to 3.10 for unburned areas samples (transitional and unburned areas), showing that Si release rate was generally smaller in the burned area samples relative to the unburned samples (Fig. 7b).

There were some differences of dissolution rates observed among the burned area samples (Bs1, Bs2 and Bs3) (Fig. 7, Supplementary Table S2). Negative correlation relationships ($r = 0.48$, $n = 20$, $p = 0.03 < 0.05$) existed between the slope coefficients of functions (fitted to relationships between DSi release and extraction days) and the carbon content of phytolith samples.

Discussion

Fire effects on phytolith morphology and assemblages

The proportion of darkened phytolith varied between plant species and could be due to the differing combustion intensity and completeness of each plant fuel^{59,60}. Fuel characteristics are also influenced by texture, surface and composition characteristics of the plant tissues. The complete combustion of some plant leaves could cause the phytolith absorbed less black carbon and low proportions of burned phytolith²⁸. The burned phytolith morphotypes were present in these plant ashes supported the darkened phytoliths gave accurate results for freshly burned material^{18,21}. However, the blackish color does not necessarily reflect heating. Some investigators believed blacken phytolith can be phytoliths extracted from reference plant material through wet oxidation^{22,61,62}. Furthermore, Wilding et al.⁶³ suggested that the blackish color observed on some fossil phytoliths can also be an iron or manganese coating. The burned and unburned blacken of phytolith in soils and sediments could be

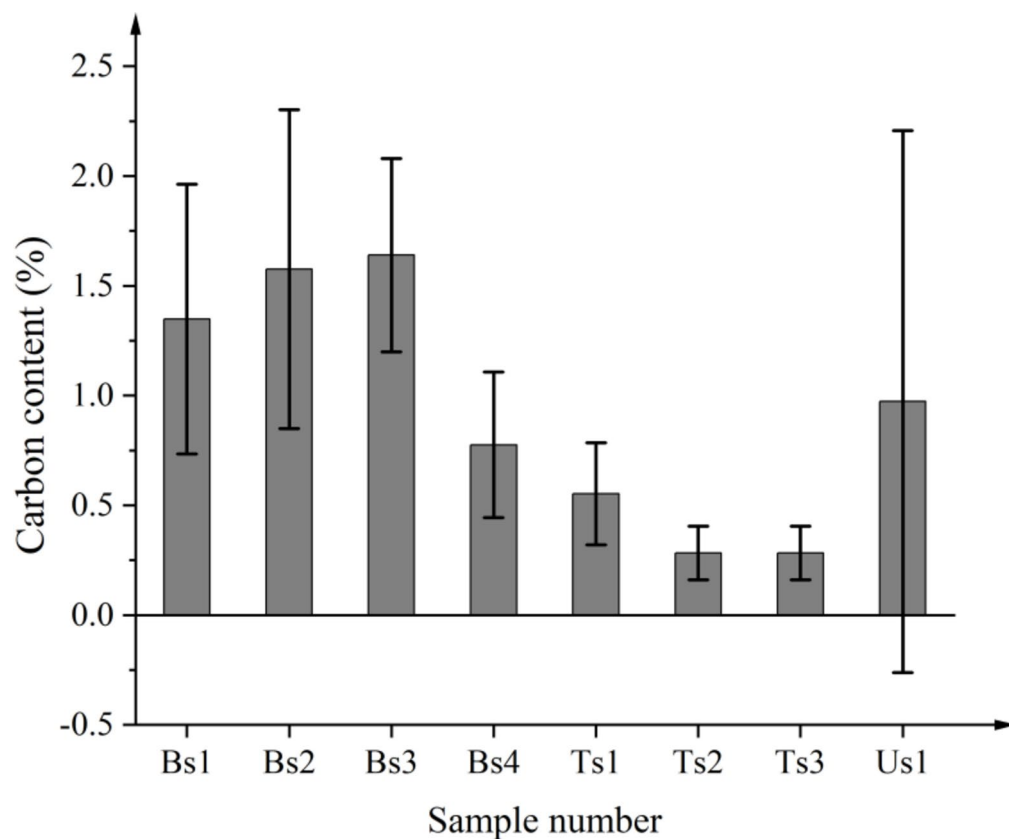


Fig. 5. Carbon content of phytolith samples from the forest fire burned area (Bs1, Bs2, Bs3, Bs4), transitional area (Ts1, Ts2, Ts3) and unburned area (Us1).

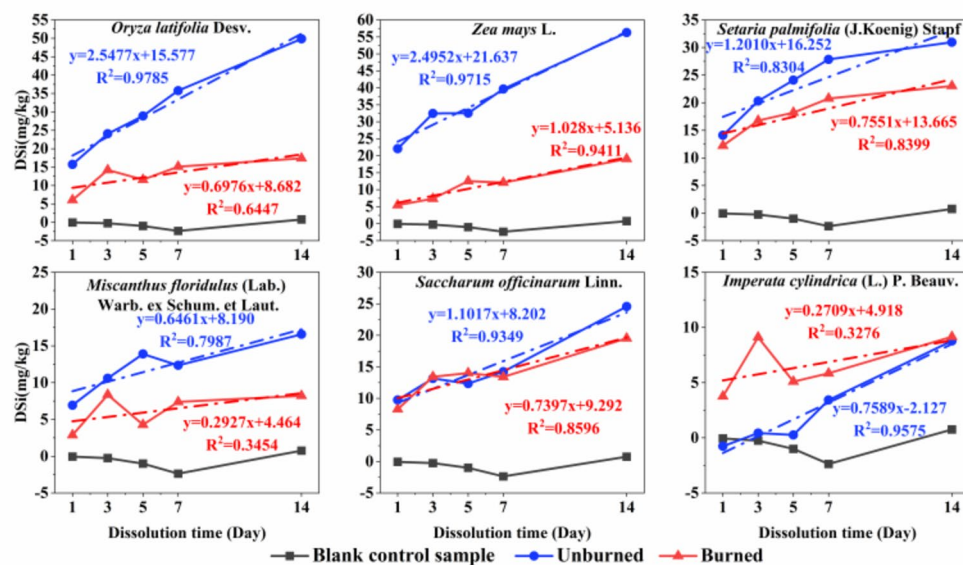


Fig. 6. Dissolved silicon release rate of unashed and ashed phytoliths from 6 grass species, as a function of time subjected to successive extraction treatments with 0.01 M CaCl₂. Note: Red = burned phytolith; Blue = unburned phytolith; Black = Blank control.

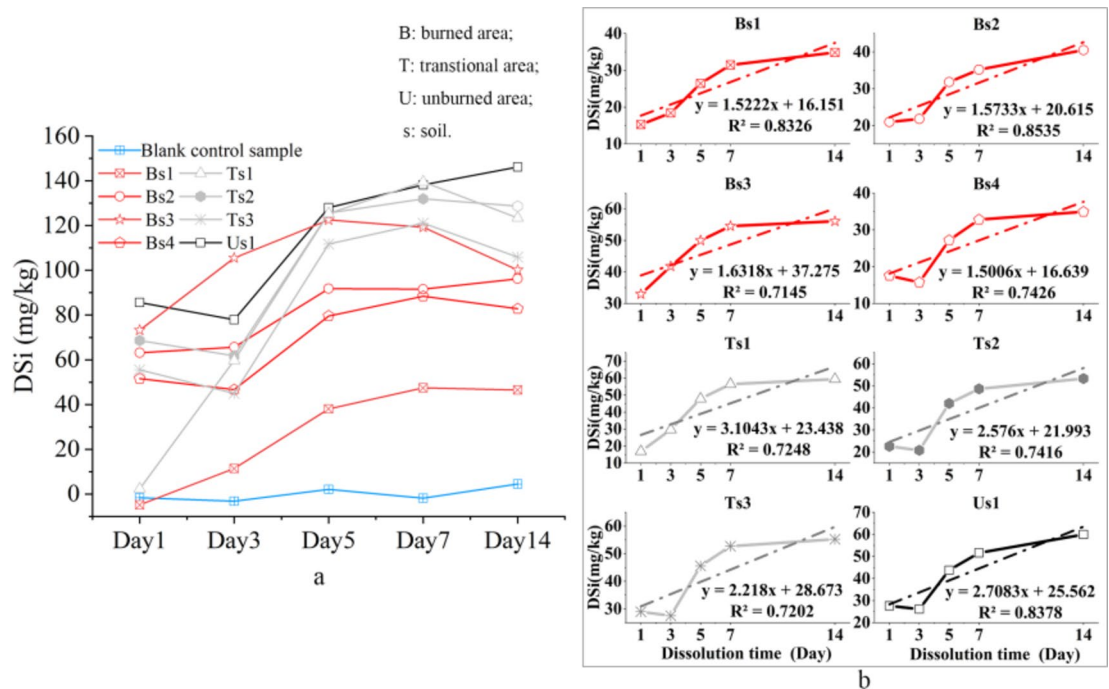


Fig. 7. Dissolved silicon release rate of the phytolith in topsoil samples from forest fire burned, unburned, and transitional areas as a function of time subjected to successive extractions with 0.01 M CaCl_2 .

distinguished with its occluded carbon content or composition detection signal if the blacken color is from carbon adsorbed during the combustion²⁸.

The sampled forest vegetation was well represented by the topsoil phytolith assemblages. The dominant BLOCKY IRREGULAR, TABULAR ELONGATE UNSCULPTED with BLOCKY SCROBICULATE, BLOCKY RIDGED are characteristic of coniferous plants^{34,47,51,64,65}. The TABULAR IRREGULAR and TRIANGULAR PRISMATIC are produced from broad leaved plants^{49,66}, and pteridophytes⁶⁵, respectively. These two morphotypes of phytoliths were also dominant, correctly indicating that they dominate the vegetation of the pine forest. The sediment samples from the burned area had greater proportions of BULLIFORM FLABELLATE, SADDLE, ELONGATE relative to the soil samples from the same area, suggesting that grass phytoliths were over represented in these soils due to taphonomic processes. BILOBATE is the major phytolith morphotype of the GSSCP and reflects the grass *Panicoidae* species that is widely distributed in southeast Asia tropical areas. Broadly, the vegetation recorded by the soil phytoliths in this study was consistent with a secondary coniferous forest composed of *Pinus massoniana* Lamb, *Quercus L. Cunninghamia lanceolata* (Lamb.) Hook (*Chinese fir*) and fern species. The fire had no apparent effects on phytolith morphologies and assemblages in topsoil from forest fire area, besides the increased proportions of microcharcoal particles^{19,47}.

Fire increases the carbon content of phytolith

There is a controversial discussion on how to determine the carbon content of phytoliths (over-extraction vs. under-extraction)⁶⁷. Santos and Alexandre⁶⁸ worry that the high PhytOC values may derive from remnant organic contaminants on the surface of extracted phytoliths. Song et al.¹³ considered that the low PhytOC values were caused by oxidation and over-extraction. The PhytOC of 0.2–1.3% for six modern plant species were low relative to the high value range (0.2–5.8%, referred to^{16,29}), and were also relatively low when compared the values reported for the same species (as examples, 1.93–2.46% for rice⁵⁵, 3.88–12.35% for sugarcane²⁶) was resulted from the increased temperature of our microwave digestion and the two-step oxidation of phytoliths with $\text{K}_2\text{Cr}_2\text{O}_7$ ²⁸. The inner OC (here PhytOC) might be decomposed at lower rates³⁸. As a result, the carbon content of phytolith should decrease because of the decomposition of its inner organic matter. However, the carbon content in ashed phytolith samples showed higher values relative to the PhytOC in modern plants and the ashed phytolith with bleaching samples. This result can be explained by carbon adsorbing to phytoliths exposed to open flames²⁸. Although fire and heat normally decompose extraneous organic matter and increase surface exposure of phytolith to cause increased phytolith solubility, our data showed the phytoliths ashed under open conditions had decreased solubility, suggesting the black carbon adsorbed by phytolith caused this decrease. A similar experiment demonstrated that the surface charge of ashed phytolith samples derived from open burning determines the adsorption/retention of elemental arsenic onto the phytolith surface¹⁷.

The PhytOC content of topsoil can also vary between microhabitats as a function of vegetation type, topography, and soil physicochemical properties because these factors influence the input, transportation, and preservation of phytolith^{13,16,53}. In this study, all sampling points were from the same sandstone soil, and were deemed to have similar physicochemical properties except for pH. The lack of correlation between pH and

phytolith carbon content suggests that soil pH has little effect on the carbon content of phytoliths. PhytOC differs between plant species because they produce variable phytolith morphotypes and assemblages^{9,25,54}. Differences in topsoil phytolith carbon content between the burned and the unburned areas could reflect the influence of local community compositions of vegetation and micro-topography on phytolith assemblages. Although cell wall phytoliths have considerably higher carbon concentrations than lumen types, the relationship between carbon content and phytolith assemblage is difficult to resolve^{9,29,67}. Us1, Ts3, Bs3 have nearly the same phytolith assemblages and corresponding vegetation, but have different carbon contents. Thus, the carbon content variations of samples between burned and unburned areas cannot be attributed to vegetation inputs or phytolith preservation. In addition, wind transportation probably mixes ashed phytolith and microcharcoal distributions between the burned and transitional/unburned areas⁴⁷. Sample Us1 from the unburned area is located northeast of the burned area, and perpendicular to the prevailing northeast wind, and covered by thick litters. Therefore, it is reasonably believed that fire had less effect on the phytoliths of Us1 than for other samples. Although samples from the transitional area (Ts1 and Ts2) are downwind, the sampling sites were covered with thick litter which could have acted like a mat to prevent ashed phytolith and microcharcoal particles from penetrating into the soils. Furthermore, they are located on the leeward slope where forest vegetation is closed, thereby reducing the input of ashed phytolith and microcharcoal particles into the forest soils. Therefore, in-situ deposition of ashed phytolith and microcharcoal likely resulted in their highest concentrations resulting in the burned area. The increased phytOC values of topsoils from the burned area might have resulted from the contribution of ashed phytolith with adsorbed black carbon. However, the darkened burned phytolith varied with phytolith morphotype and the plant species burned. There would be variability in carbon adsorption of burned phytoliths due to their specific plant morphotypes. Meanwhile, the forest fire temperature differs with their vegetation composition. It is limited to know how the carbon adsorption of burnt phytoliths change with the temperature of plant burning and forest fire. This concern needs to test the variability carbon adsorption of phytoliths from different plant burning ashes and forest fire topsoil.

Fire decreases phytolith solubility

Phytolith solubility is influenced by its SSA (specific surface area), morphology, chemical composition, and the taphonomic conditions to which it has been subjected^{13,17,39,41,69}. As different plant species produce phytolith with different morphologies, assemblages, and chemical compositions, the phytoliths from our plant leaf samples exhibit variable solubilities. Phytoliths with different dissolution rates coexist in soil: quickly dissolved fresh phytoliths and slowly dissolved aged ones. The CaCl₂ extracted-Si is considered to be controlled by the pool of fresh phytoliths in soil¹⁵. The phytoliths of the 6 plant leaves we analyzed showed decreased solubility after open burning, suggesting that the adsorption of black carbon decreased their surface exposure and thereby protected the phytolith by increasing its hydrophobicity. The negative correlation of DSI release rate with carbon content also demonstrates that the carbon content influenced the dissolution of ashed phytolith. Alternatively, rising temperatures could cause dehydroxylation of the silanol group, leading to more siloxane bonds and a more hydrophobic surface with reduced adsorption of water molecules and the prevention of siloxane bond rupture⁴². However, the Si dissolution of plants ashed in a furnace (phytoliths mixed with ash) and bio-char typically increased with temperature due to organic matter decomposition which increased the surface exposure of phytolith silica and decreased beyond a certain temperature because of the increased crystallization of phytolith^{12,17,31,38,43}. These reports are at odds with our results but can be reconciled as follows: Firstly, the reported samples were always treated in a furnace through a series of increasing temperatures. The samples would have been oxidized homogeneously and ashed completely when the furnace temperature was set to a high value (for example, 550 °C). Secondly, the furnace-treated samples would be less disturbed than phytoliths burned in situ. The homogeneous, complete, and in situ ash process will be conducive to decreasing the adsorption of black carbon, and increasing the surface exposure of phytolith. Further, more black carbon would be produced and adsorbed by phytolith in an open fire because of heterogeneous burning conditions (such as temperature, humidity, airflow, micro-topography etc.). In addition, the ashes of plant and soil organic matter contain not only phytolith silica, but also plant dissolved silicon, or other bio-silica which might be involved in the thermal reaction. Soil organic matter ash probably includes other bASi (biogenic amorphous silica) pools including protistic bASi (produced by protists), bacterial bASi (produced by bacteria), fungal bASi (produced by fungi), phytogenic bASi (produced by plants), and zoogenic bASi (formed in animals)⁷⁰. The size, surface and/or elemental compositions of these different bASi pools could cause the dissolution rate of ashed phytolith to increase, as has been reported by some researchers^{17,39,43}. Furthermore, dissolved Si in ash and bio-char is not only represented by the extractable phytoliths but also fragile silica structures, as the majority of phytolith might be stored in fragile silica structures⁷¹. Thus, it is possible and reasonable that phytolith ashed in open fire adsorbs black carbon and decreases the solubility of the phytolith. Future work will study the corresponding balance between phytolith dissolution and release of C.

Phytolith solubility varied with between plant species^{39,55,72}. Like we discussed for carbon content, the local plant community composition and micro-topography may influence each sample's phytolith assemblage, and could thereby cause its solubility to differ between burned and unburned areas. Samples from the burned area did not have lower phytolith solubility compared to those from unburned areas before 5 days. This can be explained by the presence of two different pools in a sample, ashed phytoliths and un-ashed phytoliths. The un-ashed phytoliths have similar solubility and dominate the samples collected from 1 to 2 cm depth of the soil surface. Thus, the dissolution of Si content before the fifth day is determined by the pool of un-ashed phytoliths which are input and influenced by local micro-habitats. The dissolution of Si content after 5 days is possibly controlled by the pool of ashed phytoliths. Bs1 was located on the top of the mountain which has more open conditions and drier organic matter relative to other burned samples. The temperature range of a typical vegetation fire is 600–900 °C, so phytolith exposed to temperatures higher than 500 °C for several hours

will therefore be easily identified as burnt⁷⁰. While at higher temperatures, Si crystallization of amorphous Si is observed, potentially lowering Si availability¹¹. Therefore, phytoliths of Bs1 are probably partly crystallized and have lower Si dissolution because of the ventilated conditions and dry fuels that characterized their combustion.

However, ashes contain immediately available alkali ions as well as phytolith-occluded alkali ions⁷³. Burning and resulting burned products (ashes) can therefore increase the soil pH, which may cause phytolith dissolution and a subsequent decrease of phytolith carbon sequestration⁷³. Our results especially highlight the need for further work focusing on how soil pH affects phytolith preservation following a forest fire to disentangle the combined effects of pH and black carbon adsorption.

Fire effects on phytolith carbon sequestration and its implications

PhytOC is a form of long-term carbon sequestration in soils²⁵. Although a small quantity of PhytOC can be decreased by thermal decomposition³⁸, open fire can cause phytolith to adsorb black carbon and increase its carbon content. The solubility rate of phytolith is related to phytolith preservation and carbon sequestration^{10,39,41}. The black carbon adsorption of phytolith ashed in an open fire also further decreases solubility. Black carbon adsorbed to phytolith is recalcitrant to oxidation and dissolution, and so is thereby able to be preserved in soils and sediments, increasing soil carbon sequestration. Therefore, carbon estimation of forest fire and plant burning needs consider the fire effect on carbon content and solubility of phytolith, and phytolith carbon sequestration. As phytoliths represent the main fraction of bioavailable silicon in topsoils⁷⁴, and fire decreased the solubility of burned phytolith, we suppose the silicon release from burned phytolith should be slowed and influence the soil available silicon pool and supply to the plant after forest fire event.

Many regions and countries have banned on-site agricultural burning of straw because of views that it contributes to global CO₂ and black carbon emissions. However, it is necessary to provide data quantifying the benefits and detriments of agricultural straw burning to objectively assess bans. Recent studies have demonstrated the positive effects of burning and returning burned straw to fields to recycle nutrients^{6,12} and as a means of sequestering phytolith carbon³⁸. Here, our data revealed that phytoliths burned in an open fire can increase phytolith related-carbon content and decrease solubility rate, thereby improving carbon sequestration. The black carbon adsorbed by phytoliths during fires should be considered as a positive benefit of agricultural straw burning and quantified further to estimate the potential of phytolith to sequester carbon. In addition, phytoliths burned in an open fire had consistently higher carbon content and solubility which could prove a useful proxy for fire in paleoenvironmental records. However, due to heterogeneities between plant species, transportation, and preservation, further work is needed to study whether the phytolith-related carbon and solubility rate could serve as paleofire indicators.

Conclusions

In this study, we show that burning and heat had important effects on phytolith preserved in plant ash and topsoils in an area burned by a forest fire. Burning phytoliths in an open fire increased their carbon content and decreased their solubility, with some variability between plant species. The phytoliths preserved in topsoils in burned, transitional, and unburned areas had different black carbon contents and solubilities because of preservation variations caused by local vegetation and topography. Phytoliths had higher carbon content, and generally lower solubility in the burned area relative to unburned areas (transitional and unburned).

Open fire can cause phytolith to adsorb black carbon, thereby increasing its carbon content and decreasing its solubility. This process can improve phytolith carbon sequestration in soils. Ashes cause soil pH changes which probably influence preservation and phytolith solubility. To properly estimate the flux of atmospheric CO₂ sequestered by soil phytoliths, black carbon adsorbed by phytoliths during fires should be considered and quantified. This research suggests on-site agricultural burning of straw can have positive benefits from the standpoint of phytolith carbon sequestration.

Data availability

The datasets generated and/or analysed during the current study are available in the [Supplementary Table.docx, Supplementary Figure. docx].

Received: 31 August 2024; Accepted: 25 November 2024

Published online: 03 December 2024

References

1. Bowman, D. M. J. S. et al. Fire in the earth system. *Sci* **324** (5926), 481–484 (2009).
2. Xsue, T. et al. Open fire exposure increases the risk of pregnancy loss in South Asia. *Nat. Commun.* **12** (1), 3205 (2021).
3. Bladon, K. D., Emelko, M. B., Silins, U. & Stone, M. Wildfire and the future of water supply. *Environ. Sci. Technol.* **48** (16), 8936–8943 (2014).
4. Gannon, B. M. et al. Prioritising fuels reduction for water supply protection. *Int. J. Wildland Fire* **28** (10), 785–803 (2019).
5. Gómez-Rey, M. X., Couto-Vázquez, A., García-Marco, S., Vega, J. A. & González-Prieto, S. J. Reduction of nutrient losses with eroded sediments by post-fire soil stabilisation techniques. *Int. J. Wildland Fire* **22** (5), 696–706 (2013).
6. Schaller, J. et al. Fire enhances phosphorus availability in topsoils depending on binding properties. *Ecol. (Durham)* **96** (6), 1598–1606 (2015).
7. Bodi, M. B. et al. Wildland fire ash; production, composition and eco-hydro-geomorphic effects. *Earth-Sci. Rev.* **130**, 103–127 (2014).
8. Liu, H., Zhang, L., Han, Z., Xie, B. & Wu, S. The effects of leaching methods on the combustion characteristics of rice straw. *Biomass Bioenergy* **49**, 22–27 (2013).
9. Hodson, M. J. The development of phytoliths in plants and its influence on their chemistry and isotopic composition. Implications for palaeoecology and archaeology. *J. Archaeol. Sci.* **68**, 62–69 (2016).

10. Li, R., Wen, M., Tao, X., Liu, Y. & Li, C. Advance of study on chemical composition of phytolith. *Quaternary Sci.* **40** (01), 283–293 (2020).
11. Xiao, X., Chen, B. & Zhu, L. Transformation, morphology, and dissolution of silicon and carbon in rice straw-derived biochars under different pyrolytic temperatures. *ENVIRON. SCI. TECHNOL.* **48** (6), 3411–3419 (2014).
12. Nguyen, M. N. et al. Release of potassium accompanying the dissolution of rice straw phytolith. *Chemosphere (Oxford)*. **119**, 371–376 (2015).
13. Song, Z., Liu, H., Strömberg, C. A. E., Yang, X. & Zhang, X. Phytolith carbon sequestration in global terrestrial biomes. *Sci. Total Environ.* **603–604**, 502–509 (2016).
14. Nguyen, T. N. et al. Encapsulation of lead in rice phytoliths as a possible pollutant source in paddy soils. *Environ. Exp. Bot.* **162**, 58–66 (2019).
15. Linden, C. V., Li, Z., Iserentant, A., Ranst, E. V. & Delvaux, B. Rainfall is the major driver of plant Si availability in perudic gibbsitic andosols. *Geoderma* **404** (3), 115295 (2021).
16. Song, Z. et al. High potential of stable carbon sequestration in phytoliths of China's grasslands. *Global Change Biol.* **28** (8), 2736–2750 (2022).
17. Nguyen, M. N. et al. Thermal induced changes of rice straw phytolith in relation to arsenic release: a perspective of rice straw arsenic under open burning. *E3 J. Environ. Res. Manage.* **304**, 114294 (2022).
18. Parr, J. F. Effect of fire on phytolith coloration. *Geoarchaeol* **21** (2), 171–185 (2006).
19. Morris, L. R., Ryel, R. J. & West, N. E. Can soil phytolith analysis and charcoal be used as indicators of historic fire in the pinyon-juniper and sagebrush steppe ecosystem types of the Great Basin Desert, USA? *Holocene* **20** (1), 105–114 (2010).
20. Wu, Y., Yang, Y., Wang, H. & Wang, C. The effects of chemical composition and distribution on the preservation of phytolith morphology. *Appl. Phys. Mater. Sci. Process.* **114** (2), 503–507 (2014).
21. Evett, R. R. & Cuthrell, R. Q. Testing phytolith analysis approaches to estimate the prehistoric anthropogenic burning regime on the central California coast. *Quatern Int.* **434**, 78–90 (2017).
22. Devos, Y., Hodson, M. J. & Vrydaghs, L. Auto-fluorescent phytoliths: a New Method for detecting heating and fire. *Environ. Archaeol.* **26** (40), 388–405 (2021).
23. Sarret, G. et al. Chemical status of zinc in plant phytoliths: impact of burning and (paleo)environmental implications. *Sci. Total Environ.* **852**, 158460 (2022).
24. Jones, J. B. & Segnit, E. R. Water in sphere-type opal. *MINERAL. MAG.* **37**, 357–361 (1969).
25. Parr, J. F. & Sullivan, L. A. Soil carbon sequestration in phytoliths. *Soil. Biol. Biochem.* **37** (1), 117–124 (2005).
26. Parr, J., Sullivan, L., Chen, B., Ye, G. & Zheng, W. Carbon bio-sequestration within the phytoliths of economic bamboo species. *Global Change Biol.* **16** (10), 2661–2667 (2010).
27. Alexandre, A. et al. Direct uptake of organically derived carbon by grass roots and allocation in leaves and phytoliths: 13 C labeling evidence. *Biogeosciences* **13** (5), 1693–1703 (2016).
28. Dong, H. et al. Burned phytoliths absorbing black carbon as a potential proxy for paleofire. *Holocene* **32** (5), 442–450 (2022).
29. Li, R. et al. Phytolith-occluded carbon in leaves of *Dendrocalamus Ronganensis* influenced by drought during growing season. *Physiol. Plantarum.* **174**, e1374 (2022).
30. Meng, M. et al. Characteristics of burned phytolith from representative plants in Northeast China and implications for paleo-fire reconstruction. *Rev. Palaeobot Palyno.* **300**, 104628 (2022).
31. Trinh, T. K. et al. Characterization and dissolution properties of phytolith occluded phosphorus in rice straw. *Soil. Tillage Res.* **171**, 19–24 (2017).
32. Meena, V. D. et al. A case for Silicon Fertilization to improve crop yields in Tropical soils. *Proc. Natl. Acad. Sci. India Sect. B Biol. Sci. : Biol. Sci.* **84** (3), 505–518 (2014).
33. Yang, X. et al. Phytolith-rich straw application and groundwater table management over 36 years affect the soil-plant silicon cycle of a paddy field. *Plant. Soil.* **454** (1–2), 1–16 (2020).
34. Piperno, D. R. Phytoliths: a comprehensive guide for archaeologists and paleoecologists. (2006). <https://doi.org/10.5860/choice.4.4-0942>
35. Zuo, X. et al. Dating rice remains through phytolith carbon-14 study reveals domestication at the beginning of the Holocene. *P Natl. Acad. Sci. USA.* **114** (25), 6486–6491 (2017).
36. Reyerson, P. E. et al. Unambiguous evidence of old soil carbon in grass biosilica particles. *Biogeosciences* **13** (4), 1269–1286 (2016).
37. Zhang, X. et al. The impact of different forest types on phytolith-occluded carbon accumulation in subtropical forest soils. *J. Soils Sediments.* **16** (2), 461–466 (2016).
38. Nguyen, A. T. Q. & Nguyen, M. N. Straw phytolith for less hazardous open burning of paddy straw. *Sci. Rep-UK.* **9** (1), 20043 (2019).
39. Cabanes, D., Weiner, S. & Shahack-Gross, R. Stability of phytoliths in the archaeological record: a dissolution study of modern and fossil phytoliths. *J. Archaeol. Sci.* **38** (9), 2480–2490 (2011).
40. Li, Z., de Tombeur, F., Linden, C. V., Cornelis, J. & Delvaux, B. Soil microaggregates store phytoliths in a sandy loam. *Geoderma* **360**, 114037 (2020).
41. Liu, H. et al. Dissolution does not affect grass phytolith assemblages. *Palaeogeogr Palaeoclimatol Palaeoecol.* **610**, 111345 (2023).
42. Zhuravlev, L. T. The surface chemistry of amorphous silica. Zhuravlev model. *Colloids Surf. A: Physicochemical Eng. Aspects.* **173** (1), 1–38 (2000).
43. Unzué-Belmonte, D. et al. Fire enhances solubility of biogenic silica. *Sci. Total Environ.* **572**, 1289–1296 (2016).
44. Wang, Y., Xiao, X., Xu, Y. & Chen, B. Environmental effects of Silicon within Biochar (Sichar) and Carbon–Silicon Coupling mechanisms: a critical review. *Environ. Sci. Technol.* **53** (23), 13570–13582 (2019).
45. Qader, W., Dar, R. A. & Rashid, I. Phytolith particulate matter and its potential human and environmental effects. *Environ. Pollut.* **327**, 121541 (2023).
46. Li, R., Meyers, P. A., Fan, J. & Xue, J. Monthly changes in chain length distributions and stable carbon isotope composition of leaf nalkanes during growth of the bamboo *Dendrocalamus ronganensis* and the grass *Setaria viridis*. *Org. Geochem.* **101**, 72–81 (2016).
47. Wen, M. et al. The ratio of microcharcoal to phytolith content in soils as a new proxy of fire activity. *Holoc (Sevenoaks)*. **30** (11), 1612832284 (2020).
48. Blackford, J. J. Charcoal fragments in surface samples following a fire and the implications for interpretation of subfossil charcoal data. *Palaeogeogr Palaeoclimatol Palaeoecol.* **164** (1), 33–42 (2000).
49. Li, R., Fan, J., Vachula, R. S., Tan, S. & Qing, X. Spatial distribution characteristics and environmental significance of phytoliths in surface sediments of Qingshitian Lake in Southwest China. *J. Paleolimnol.* **61** (2), 201–215 (2019).
50. Li, R., Fan, J., Carter, J., Jiang, N. & Gu, Y. Monthly variations of phytoliths in the leaves of the bamboo *Dendrocalamus ronganensis* (Poaceae: Bambusoideae). *Rev. Palaeobot Palyno.* **246**, 62 (2017).
51. Hu, M. et al. The identification of phytolith characteristics of the herbaceous and woody plants in northeast China. *Acta Micropalaeontol Sin.* **35** (02), 122–139 (2018).
52. Neumann, K., Strömberg, C. A. E., Ball, T., Vrydaghs, R. M. A., Cummings, L. S. & L. & International Code for Phytolith nomenclature (ICPN) 2.0. *Ann. Bot-London.* **124** (2), 189–199 (2019).
53. Yang, X. et al. Topographic control on phytolith carbon sequestration in moso bamboo (*Phyllostachys pubescens*) ecosystems. *Carbon Manage.* **7** (1–2), 105–112 (2016).

54. Li, Z., Song, Z., Parr, J. F. & Wang, H. Occluded C in rice phytoliths: implications to biogeochemical carbon sequestration. *J. Plant. Nutr. Soil. Sci.* **370** (1–2), 615–623 (2013).
55. Li, Z., Song, Z. & Cornelis, J. Impact of rice cultivar and organ on elemental composition of phytoliths and the release of bio-available silicon. *Front. Recent. Dev. Plant. Sci.* **5**, 529 (2014).
56. Sauer, D., Saccone, L., Conley, D. J., Herrmann, L. & Sommer, M. Review of methodologies for extracting plant-available and amorphous Si from soils and aquatic sediments. *Biogeochemistry* **80**, 89–108 (2006).
57. Fishman, M. J. & Friedman, L. C. Methods for determination of inorganic substances in water and fluvial sediments. *Techniques of Water-resources Investigations of The United States Geological Survey* (1989).
58. Wang, J., Liu, L., Gao, Z. & Jie, D. Effects of available soil silicon on the formation of phytoliths in *Phragmites australis* (Cav.) Trin. Ex Streud, Poaceae. *Bot. Lett.* **166**(1), 51–63 (2018).
59. Hudspith, V. A., Hadden, R. M., Bartlett, A. I., Belcher, C. M. & Seyfullah, L. Does fuel type influence the amount of charcoal produced in wildfires? Implications for the fossil record. *Dev. Palaeontol. Stratigr.* **61** (2), 159–171 (2018).
60. Lennox, S. J. & Wadley, L. A charcoal study from the Middle Stone Age, 77,000 to 65,000 years ago, at Sibudu, KwaZulu-Natal. *Trans. R Soc. S Afr.* **74** (1), 38–54 (2019).
61. Piperno, D. R. *Phytolith Analysis: An Archaeological and Geological Perspective* (Academic, 1988).
62. Piperno, D. R. & Phytoliths *A Comprehensive Guide for Archaeologists and Paleoecologists* (Altamira, 2006).
63. Wilding, L. P., Brown, R. E. & Holowaychuk, N. Accessibility and Properties of Occluded Carbon in Biogenetic Opal. *Soil. Sci.* **10**, 56–61 (1967).
64. Barboni, D., Bonnefille, R., Alexandre, A. & Meunier, J. D. Phytoliths as paleoenvironmental indicators, West Side Middle Awash Valley, Ethiopia. *Palaeogeogr Palaeoclimatol Palaeoecol.* **152** (1), 38–54 (1999).
65. Liu, L. et al. Representativeness of soil phytoliths for plant communities in the forest and grassland regions of Northeast China. *Disiji Yanjiu.* **40**, 1285–1300 (2020).
66. Gao, G. et al. Phytolith reference study for identifying vegetation changes in the forest-grassland region of northeast China. *Boreas* **47** (2), 481–497 (2018).
67. Hodson, M. J. The relative importance of Cell Wall and Lumen Phytoliths in Carbon Sequestration in Soil: a hypothesis. *Front. Environ. Sci.* **7**, 167 (2019).
68. Santos, G. M. & Alexandre, A. The phytolith carbon sequestration concept: fact or fiction? A comment on occurrence, turnover and carbon sequestration potential of phytoliths in terrestrial ecosystems by Song. *Earth-Sci. Rev.* **164**, 251–255. <https://doi.org/10.1016/j.earscirev.2016.04.007> (2017).
69. Koebernick, N., Mikutta, R., Kaiser, K., Klotzbücher, A. & Klotzbücher, T. Redox-dependent surface passivation reduces phytolith solubility. *Geoderma* **428**, 116158 (2022).
70. Puppe, D. Review on protozoic silica and its role in silicon cycling. *Geoderma* **365**, 114224 (2020).
71. Puppe, D., Kaczorek, D., Buhtz, C. & Schaller, J. The potential of sodium carbonate and Tiron extractions for the determination of silicon contents in plant samples—A method comparison using hydrofluoric acid digestion as reference. *Front. Environ. Sci.* **11**, 1145604 (2023).
72. Wilding, L. P. & Drees, L. R. Contributions of forest opal and associated crystalline phases to fine silt and clay fractions of soils. *Clays Clay Min.* **22** (3), 295–306 (1974).
73. Nguyen, M. N., Dultz, S. & Guggenberger, G. Effects of pretreatment and solution chemistry on solubility of rice-straw phytoliths. *J. Plant. Nutr. Soil. Sci.* **177** (2), 217–226 (2014).
74. Cornelis, J. T., Ranger, J., Iserentant, A. & Delvaux, B. Tree species impact the terrestrial cycle of silicon through various uptakes. *Biogeochemistry* **97**, 231–245 (2010).

Acknowledgements

We are grateful to Xiaobei Wei, Baifeng Cao, Cuiyu Wei and Tianxi Gan for help during the sampling and experiment.

Author contributions

RC Li: Supervision, conceptualization, validation, formal analyses, writing -original draft, funding acquisition. ZT Gu: Investigation, methodology, Software, Data curation. RS Vachula: Conceptualization, writing - reviewing and editing. HY Dong: Investigation, methodology, data curation, conceptualization. MT Xu, XF Chen, B Xu and YW Sun: Conceptualization, writing - reviewing and editing. All authors contributed to the article and approved the submitted version.

Declarations

Competing interests

The authors declare no competing interests.

Additional information

Supplementary Information The online version contains supplementary material available at <https://doi.org/10.1038/s41598-024-81246-9>.

Correspondence and requests for materials should be addressed to R.L. or H.D.

Reprints and permissions information is available at www.nature.com/reprints.

Publisher's note Springer Nature remains neutral with regard to jurisdictional claims in published maps and institutional affiliations.

Open Access This article is licensed under a Creative Commons Attribution-NonCommercial-NoDerivatives 4.0 International License, which permits any non-commercial use, sharing, distribution and reproduction in any medium or format, as long as you give appropriate credit to the original author(s) and the source, provide a link to the Creative Commons licence, and indicate if you modified the licensed material. You do not have permission under this licence to share adapted material derived from this article or parts of it. The images or other third party material in this article are included in the article's Creative Commons licence, unless indicated otherwise in a credit line to the material. If material is not included in the article's Creative Commons licence and your intended use is not permitted by statutory regulation or exceeds the permitted use, you will need to obtain permission directly from the copyright holder. To view a copy of this licence, visit <http://creativecommons.org/licenses/by-nc-nd/4.0/>.

© The Author(s) 2024